# Direct Torque Control of Brushless DC Drives with Reduced Torque Ripple

Y. Liu, Z.Q. Zhu, D. Howe
Department of Electronic and Electrical Engineering,
University of Sheffield, Mappin Street,
Sheffield S1 3JD, UK

*Abstract*— **The application of direct torque control (DTC) to brushless AC drives (BLAC) has been investigated extensively. This paper describes its application to brushless DC drives (BLDC), and highlights the essential differences in its implementation, as regards torque estimation and the representation of the inverter voltage space vectors. Simulated and experimental results are presented, and it is shown that, compared with conventional current control, instantaneous torque control results in reduced torque ripple and a faster torque response.**

***Keywords-Direct Torque Control; Brushless DC Drives; Permanent Magnet Motor***

## I. INTRODUCTION

BLDC drives commonly employ current control, which essentially assumes that the torque is proportional to the phase current. However, since, in practice, the relationship is nonlinear, various current control strategies have been adopted to minimize torque pulsations, by employing pre-optimised waveforms for the current reference, for example. Such an optimal current excitation scheme was proposed in [1], which resulted in minimal copper loss and ripple-free torque from a BLDC drive. However, it was based on the d-q axis transformation, and could not respond to rapid torque changes. A conventional current controller, which estimated the electromagnetic torque from the rate of change of coenergy, was described in [2]. However, in its implementation to a BLDC drive, the estimated torque was obtained from a look-up table, and the control algorithm did not directly involve flux control.

Various torque control methods have also been proposed to minimize torque pulsations. For example, an instantaneous torque controller based on variable structure control in the d-q reference frame was proposed in [3-5]. However, although experimental results showed that it was effective in reducing torque ripple, it was only applicable to three-phase conducting (i.e. 180° conduction) BLDC drives, and not to the more usual two-phase conducting (i.e. 120° conduction) BLDC drives. In [6], electromagnetic torque pulsations were reduced with a torque controller, the torque being estimated from the product of the instantaneous back-emf and current. However, the phase resistance was neglected and the inverter output voltage had to be calculated, which assumed that the back-emf waveform was known. The real-time estimation of the back-emf, using the model reference adaptive method, was reported in [7], which also employed a variable structure torque controller with space vector pulse width modulation. However, it was only applied to a 3-phase BLAC drive, and resulted in a relatively complex relationship between the output voltage in the q-axis and the torque error.

This paper considers the application of DTC to a BLDC drive operating in the two-phase conducting mode to achieve instantaneous torque control and reduced torque ripple. As will be shown, the essential differences between the DTC of BLDC drives and BLAC are in the torque calculation and the representation of the voltage space vectors. Simulated and experimental results are presented to illustrate the application of DTC to a BLDC drive.

## II. DIRECT TORQUE CONTROL OF BLAC AND BLDC DRIVES

In general, neglecting the influence of mutual coupling between the direct and quadrature axes, the electromagnetic torque of a permanent magnet brushless machine in the synchronously rotating d-q reference frame can be expressed as [7-9]:

$$T_e = \frac{3}{2}\frac{p}{2}[(\frac{dL_d}{d\theta_e}i_{sd} + \frac{d\psi_{rd}}{d\theta_e} - \psi_{sq})i_{sd} + (\frac{dL_q}{d\theta_e}i_{sq} + \frac{d\psi_{rq}}{d\theta_e} + \psi_{sd})i_{sq}] \quad (1)$$

where

$$\psi_{sd} = L_d i_{sd} + \psi_{rd} \quad (2)$$

$$\psi_{sq} = L_q i_{sq} + \psi_{rq} \quad (3)$$

and $\theta_e$ is the rotor electrical angle, $p$ is the number of poles, $i_{sd}$ and $i_{sq}$ are the d- and q-axis currents, $L_d$ and $L_q$ are the d- and q-axis inductances, respectively, and $\psi_{rd}$, $\psi_{rq}$, $\psi_{sd}$ and $\psi_{sq}$ are the d- and q-axis rotor and stator flux-linkages, respectively.

After a d-q transformation, a fundamental component is transformed into a dc component; whilst 5th and 7th harmonics transform into 6th harmonics; 11th and 13th harmonics transform into 12th harmonics; 17th and 19th harmonics transform into 18th harmonics, and so on. Thus, for a machine having a sinusoidal permanent magnet flux, $\psi_{rd}$=constant and $\psi_{rq}$=0. However, for non-sinusoidal flux $\psi_{rd}$ is composed of a dc component and 6th, 12th, 18th harmonics, etc., while $\psi_{rq}$ consists of 6th, 12th, 18th harmonics, etc.

Torque pulsations are associated mainly with the flux harmonics, the influence of higher order harmonics in the stator winding inductance usually being negligible [10]. Therefore, for machines equipped with a surface-mounted magnet rotor (i.e. non-salient), it can be assumed that $L_d$ and $L_q$ are constant, i.e. $L_d=L_{d0}$, $L_q=L_{q0}$, and the electromagnetic torque can be expressed as:

 0-7803-8486-5/04/$20.00 © 2004 IEEE

$$T_e = \frac{3}{2}\frac{p}{2}[(\frac{d\psi_{rd}}{d\theta_e} - \psi_{rq})i_{sd} + (\frac{d\psi_{rq}}{d\theta_e} + \psi_{rd})i_{sq} + (L_{d0} - L_{q0})i_{sq}i_{sd}] \quad (4)$$

At this stage, it is worth considering the following cases:

(a) When the stator flux-linkage due to the permanent magnets varies sinusoidally, $\psi_{rd}$ is constant, $\psi_{rq}$=0, $\frac{d\psi_{rd}}{d\theta_e} = 0$, and $\frac{d\psi_{rq}}{d\theta_e} = 0$. The electromagnetic torque equation, for both BLAC and BLDC operation, with either a non-salient or salient pole rotor, can then be simplified as:

$$T_e = \frac{3}{2}\frac{p}{2}(\psi_{sd}i_{sq} - \psi_{sq}i_{sd}) \quad (5)$$

or, in the stationary $\alpha$-$\beta$ reference frame, as:

$$T_e = \frac{3}{2}\frac{p}{2}(\psi_{s\alpha}i_{s\beta} - \psi_{s\beta}i_{s\alpha}) \quad (6)$$

where $i_{sa}$, $i_{s\beta}$, $\psi_{sa}$, and $\psi_{s\beta}$ are the $\alpha$- and $\beta$-axis stator currents and flux-linkages, respectively, viz.:

$$\psi_{s\alpha} = \psi_{sd}\cos\theta_e - \psi_{sq}\sin\theta_e \quad (7)$$

$$\psi_{s\beta} = \psi_{sd}\sin\theta_e + \psi_{sq}\cos\theta_e \quad (8)$$

$$i_{s\alpha} = i_{sd}\cos\theta_e - i_{sq}\sin\theta_e \quad (9)$$

$$i_{s\beta} = i_{sd}\sin\theta_e + i_{sq}\cos\theta_e \quad (10)$$

However, if the stator flux-linkage variation is non-sinusoidal, which is generally the case for BLDC machines, the general torque equation, (1) must be employed, since $\frac{d\psi_{rd}}{d\theta_e} \neq 0$, $\frac{d\psi_{rq}}{d\theta_e} \neq 0$.

(b) For non-salient pole brushless machines with a non-sinusoidal stator flux-linkage since $L_{d0} = L_{q0} = L_s$, the electromagnetic torque, for both BLAC and BLDC operation, can be simplified as:

$$T_e = \frac{3}{2}\frac{p}{2}[(\frac{d\psi_{rd}}{d\theta_e} - \psi_{rq})i_{sd} + (\frac{d\psi_{rq}}{d\theta_e} + \psi_{rd})i_{sq}] \quad (11)$$

in the rotating d-q axis reference frame, or in the stationary $\alpha$-$\beta$ reference frame as:

$$T_e = \frac{3}{2}\frac{p}{2}[\frac{d\psi_{r\alpha}}{d\theta_e}i_{s\alpha} + \frac{d\psi_{r\beta}}{d\theta_e}i_{s\beta}] \quad (12)$$

where $\psi_{ra}$ and $\psi_{r\beta}$ are the $\alpha$- and $\beta$-axis rotor flux-linkages, respectively, viz.:

$$\psi_{r\alpha} = \psi_{rd}\cos\theta_e - \psi_{rq}\sin\theta_e \quad (13)$$

$$\psi_{r\beta} = \psi_{rd}\sin\theta_e + \psi_{rq}\cos\theta_e \quad (14)$$

However, for a non-salient BLAC motor with a sinusoidal flux-linkage, $\psi_{rd} = \psi_m$ and $\psi_{rq} = 0$, and the torque equation can be further simplified as:

$$T_e = \frac{3}{2}\frac{p}{2}\psi_m i_{sq} \quad (15)$$

or, in the stationary reference frame as:

$$T_e = \frac{3}{2}\frac{p}{2}(\psi_{s\alpha}i_{s\beta} - \psi_{s\beta}i_{s\alpha}) \quad (16)$$

which is the same as equation (6).

Equation (16) is a particular case of equation (12) when the back-emf waveform is sinusoidal, or represents the fundamental component of electromagnetic torque when the back-emf waveform is non-sinusoidal. In general, equation (12) should be used to calculate the torque when the back-emf waveform is non-sinusoidal.

As with the application of DTC to BLAC drives [11], the implementation of proposed DTC to BLDC drives is based on flux-linkage observers. The stator flux-linkage vector can be obtained from the measured stator voltages, $u_{s\alpha}$, $u_{s\beta}$, and currents, $i_{s\alpha}$, $i_{s\beta}$, as:

$$\psi_{s\alpha} = \int (u_{s\alpha} - Ri_{s\alpha})dt \quad (17)$$

$$\psi_{s\beta} = \int (u_{s\beta} - Ri_{s\beta})dt \quad (18)$$

where $R$ is the stator winding resistance. The magnitude and angular position of the stator flux-linkage vector is:

$$\psi = \sqrt{\psi_{s\alpha}^2 + \psi_{s\beta}^2} \quad (19)$$

$$\theta = \arctan\frac{\psi_{s\beta}}{\psi_{s\alpha}} \quad (20)$$

The rotor flux-linkages can be deduced from the stator flux-linkages. For example, for a surface-mounted permanent magnet motor, they are given by:

$$\psi_{r\alpha} = \psi_{s\alpha} - L_s i_{s\alpha} \quad (21)$$

$$\psi_{r\beta} = \psi_{s\beta} - L_s i_{s\beta} \quad (22)$$

while the torque can be calculated from equation (12). To simplify the calculation, however, the differential terms in equation (12) can be pre-determined from the back-emf waveform assuming that the emf is proportional to the speed.

Six non-zero voltage space vectors are defined for a BLDC drive, as shown in Fig. 1(a), the divisions of the vector circle to select the voltage vector in terms of the stator flux-linkage vector being shown in Fig. 1(b). For comparison, the six non-zero voltage space vectors and the divisions of the vector circle for a BLAC drive are shown in Figs. 2(a) and 2(b), respectively. Figs. 1(c) and 2(c) show the idealized phase current waveforms for BLDC and BLAC drives, and their

relationship with voltage space vector sections and switching states.

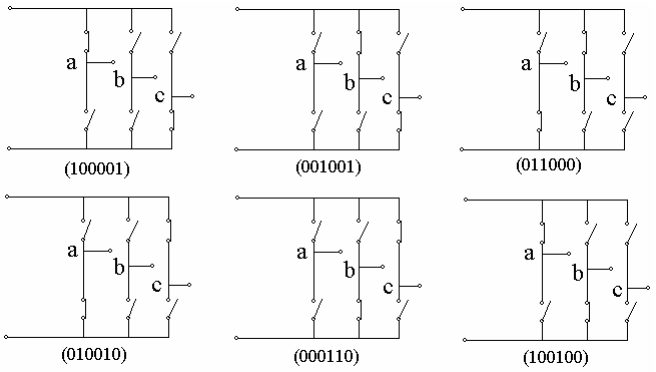


(a)

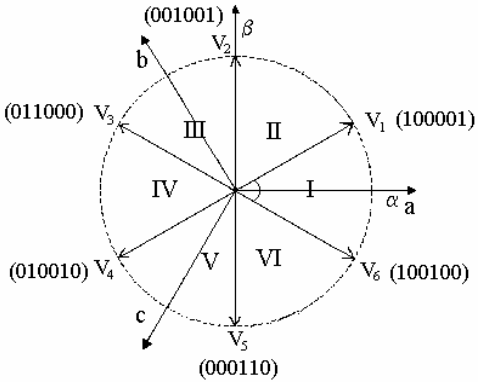


(b)

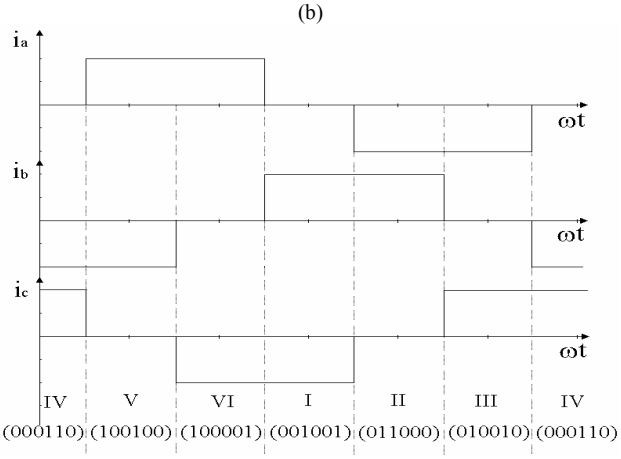


(c)

Figure 1. Non-zero voltage space vectors for BLDC drive.

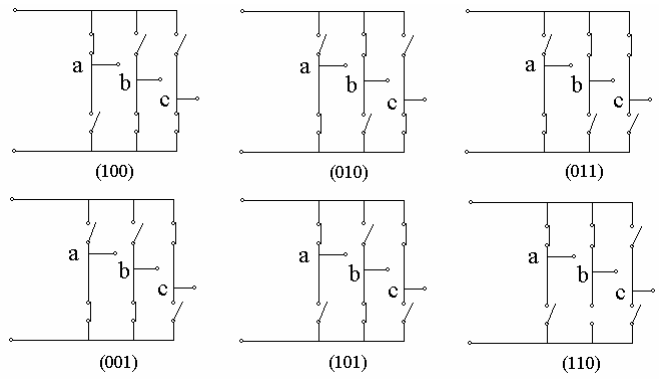


(a)

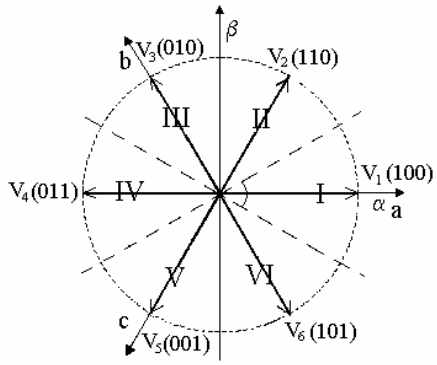


(b)

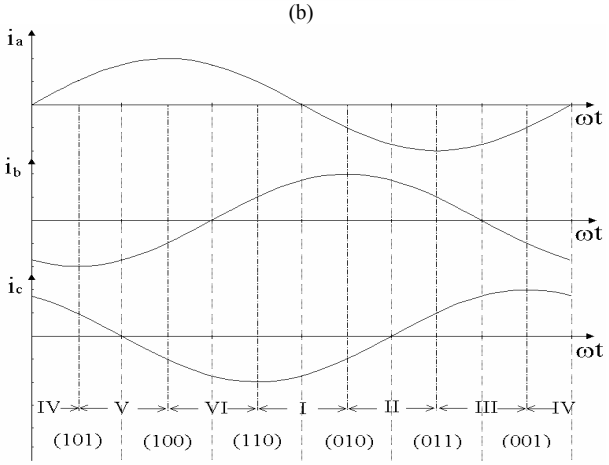


(c)

Figure 2. Non-zero voltage space vectors for BLAC drive.

From the foregoing, the main differences between the representation of the voltage space vector in BLAC and BLDC drives are:

(a) In a BLAC drive, the voltage space vectors can be represented by 3 digits, Fig. 2(a), which fully represent all the states of the inverter switches, since only one digit is required for each switching leg, as the upper and lower switches operate in tandem mode. In a BLDC drive, however, since the upper and lower switches in a phase leg may both be simultaneously off, irrespective of the state of the associated freewheel diodes, Fig. 1(a). 6 digits are required, one digit for each switch. Thus, the voltage space vectors $V_1$, $V_2$, … $V_6$ are represented as switching signals (100001), (001001), (011000), (010010), (000110), (100100), respectively, where, from left to right, the logical values express states of the upper and lower switch signals of phases A, B, and C, respectively. The zero voltage space vector is defined as (000000).

(b) The voltage space vectors in the α-β reference frame for a BLDC drive have a 30° phase difference relative to those for a BLAC drive, as will be seen by comparing Figs. 1(b) and 2(b). Two non-zero voltage space vectors now bound each section of the vector circle, as will be seen in Fig. 1(b), while in a BLAC drive each section is centered on a non-zero voltage space vector. In each section, if the actual stator flux-linkage is the same as the commanded stator flux-linkage ($\phi$=0), only one non-zero voltage space vector and a zero voltage vector are used to control the increase ($\tau$=1) and decrease ($\tau$=0) of the torque, since during any

$60^{o}$elec. period only two phases are excited and controlled in a BLDC drive, as indicated in Table I. In addition, when the actual flux-linkage is smaller than the commanded value ($\phi$=1), the non-zero voltage space vector is used to increase the flux-linkage, while when the actual flux-linkage is greater than the commanded value ($\phi$= -1), the non-zero voltage space vector which decreases the stator flux-linkage is used.

TABLE I
SWITCHING TABLE OF DTC FOR BLDC DRIVE

| Torque $\tau$ | Flux $\phi$ | Section I | II | III | IV | V | VI |
|---|---|---|---|---|---|---|---|
| 1 | 1 | $V_1$ (100001) | $V_2$ (001001) | $V_3$ (011000) | $V_4$ (010010) | $V_5$ (000110) | $V_6$ (100100) |
| | **0** | **$V_2$ (001001)** | **$V_3$ (011000)** | **$V_4$ (010010)** | **$V_5$ (000110)** | **$V_6$ (100100)** | **$V_1$ (100001)** |
| | -1 | $V_3$ (011000) | $V_4$ (010010) | $V_5$ (000110) | $V_6$ (100100) | $V_1$ (100001) | $V_2$ (001001) |
| 0 | 1 | $V_1$ (100001) | $V_2$ (001001) | $V_3$ (011000) | $V_4$ (010010) | $V_5$ (000110) | $V_6$ (100100) |
| | **0** | **$V_0$ (000000)** | **$V_0$ (000000)** | **$V_0$ (000000)** | **$V_0$ (000000)** | **$V_0$ (000000)** | **$V_0$ (000000)** |
| | -1 | $V_3$ (011000) | $V_4$ (010010) | $V_5$ (000110) | $V_6$ (100100) | $V_1$ (100001) | $V_2$ (001001) |

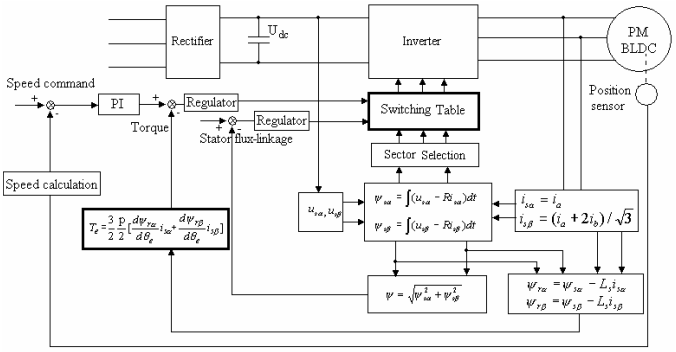


Figure 3. Block diagram for DTC of BLDC drive.

In summary, the main difference between the DTC of BLDC and BLAC drives are in the torque estimation and the representation of the inverter voltage space vectors. However, the control algorithms for the demanded torque, the stator flux-linkage and the output voltage vectors can be established in a similar manner to that for BLAC drives.

## III. SIMULATED AND EXPERIMENTAL RESULTS

The utility of the foregoing DTC method for BLDC drives has been validated on two surface-mounted permanent magnet brushless DC motors, whose parameters are given in Table II, the motors having significantly different back-emf waveforms, Figs. 5 and 6. The main elements of the DSP-based drive system are shown in Fig. 4. The controller is composed of DAC boards, ADC boards, a position board, a transducer board and a TMS320C31 DSP, on which the control algorithms are implemented in the DSP. Each DAC board has four 12-bit digital-to-analogue converter (AD767) channels, which are used to output parameters such as the motor speed and phase current. Its output port provides gate drive signals for the switching devices. Each ADC board has four 12-bit analogue-to-digital converter (AD678) channels and a 12-bit digital input parallel port. In addition, there are current transducers (LEM LA25-NP) and voltage transducers (LEM LV25-P). The phase currents, and voltages and the inverter DC link voltage are measured and sampled by the transducer board and ADC board, respectively.

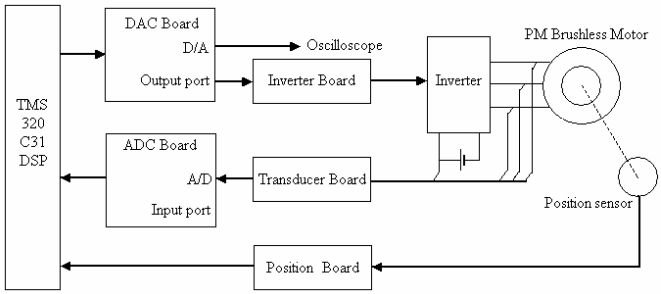


Figure 4. Schematic of BLDC drive system.

TABLE II
SPCIFICATION OF SURFACE-MOUNTED PM BRUSHLESS MOTOR

| Motor | 1 | 2 |
|---|---|---|
| Back-emf | Sinusoidal | Non-sinusoidal |
| Number of poles, p | 2 | 10 |
| DC link voltage (V) | 70 | 36 |
| Rated speed (rpm) | 3000 | 400 |
| PM excitation flux-linkage (Wb): | 0.0928 | 0.0794 |
| Phase resistance ($\Omega$) | 0.466 | 0.35 |
| Self-inductance (mH) | 3.19 | 4.64 |
| Mutual-inductance (mH) | -1.31 | 0.0023 |

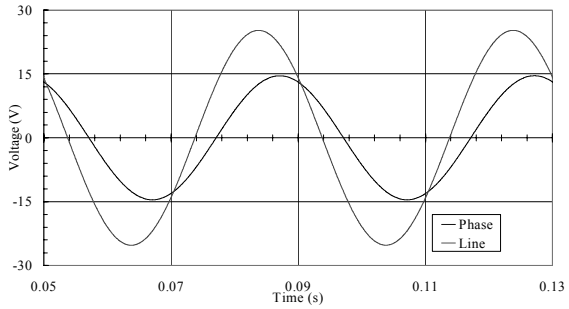


Figure 5. Back-emf waveforms of Motor 1.

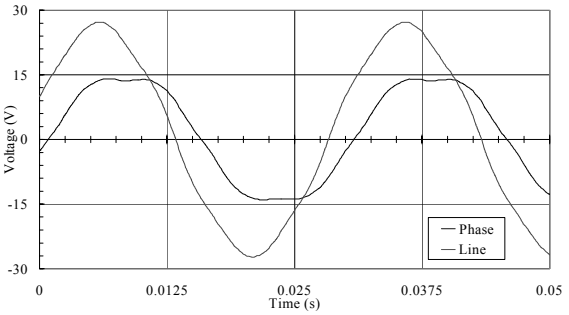


Figure 6. Back-emf waveforms of Motor 2.

The position board is simply an interface between the DSP and the rotor position sensor. DC components in the measured voltages and currents are filtered out, using a high pass filter. Equations (16) and (12) are used in the implementation of DTC for Motors 1 and 2, respectively. A simulation model has also been developed on Matlab/Simulink, and used to predict the performance of the drives. By way of example, Figs. 7-10 compare the simulated and measured phase winding terminal to ground voltage, and the phase voltage and current, as well as the locus of the stator flux-linkage, and the estimated electromagnetic torque for both motors.

As will be seen, in general, good agreement is achieved between simulated and measured results. Further, it will be seen that the phase current waveform inherently follows the inverse of the back-emf waveform within each 60° elec. sector of the 120° elec. conduction period so as to maintain the electromagnetic torque constant. In addition, it should be noted that whilst in BLAC drives the locus of the stator flux-linkage is ideally circular, in a BLDC drive it is non-circular due to the incremental rotation of the stator flux as a result of communication events, which occur every 60° elec. in a 120° elec. conduction BLDC drive. Thus, the flux-linkage locus tends to a hexagon, as for a six-step machine drive, whose sides are curved due to the influence of the back-emf of the unexcited phase and which exhibits discrete changes in amplitude every 60° elec due to the action of the free-wheeling diodes. Further, it will be noted that whilst a high frequency torque ripple exists in both the simulated and experimental results, this results from the low winding inductances and PWM events, the low frequency torque ripple which would have resulted with conventional vector control having been eliminated by optimizing the phase current waveform in accordance with the back-emf waveform.

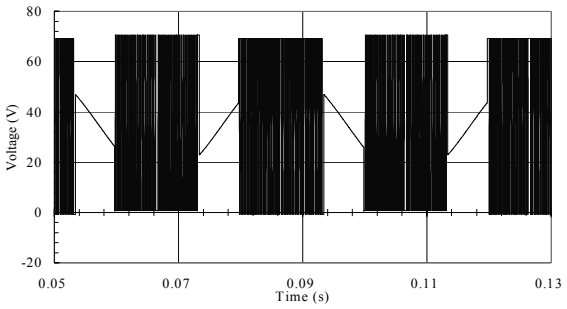


(a) Phase winding terminal to ground voltage

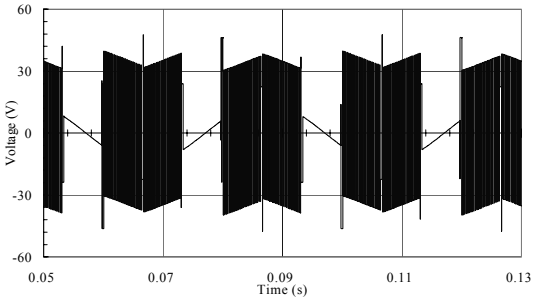


(b) Phase voltage

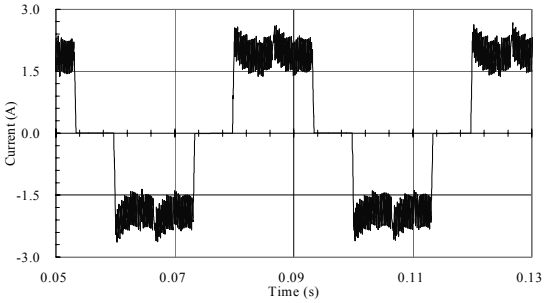


(c) Phase current

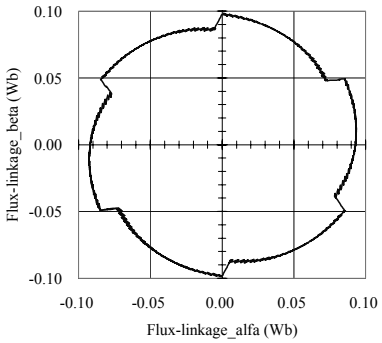


(d) Locus of stator flux-linkage

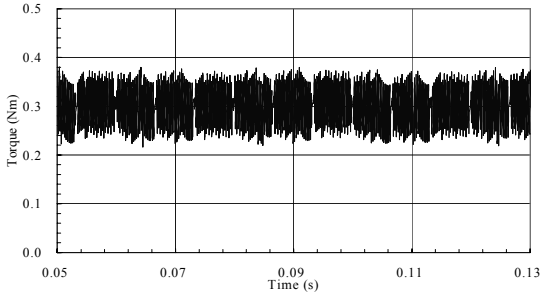


(e) Electromagnetic torque

Figure 7. Simulated results for Motor 1 (1500rpm).

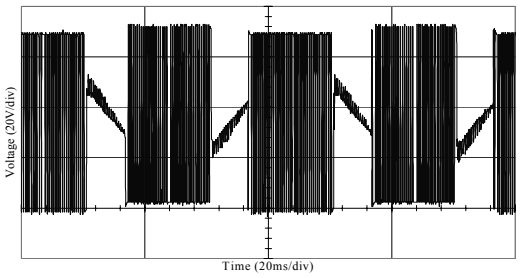


(a) Phase winding terminal to ground voltage

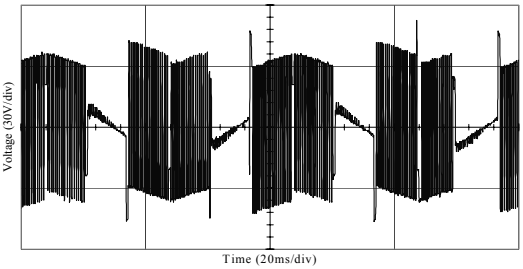


(b) Phase voltage

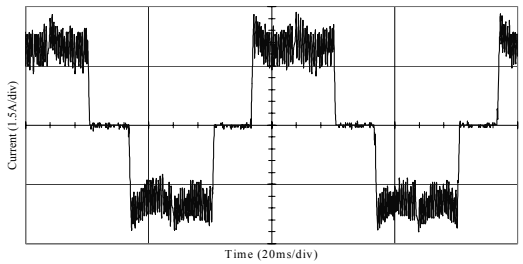


(c) Phase current

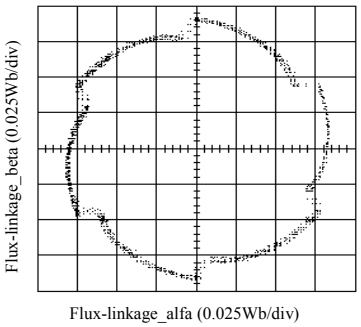


(d) Locus of stator flux-linkage

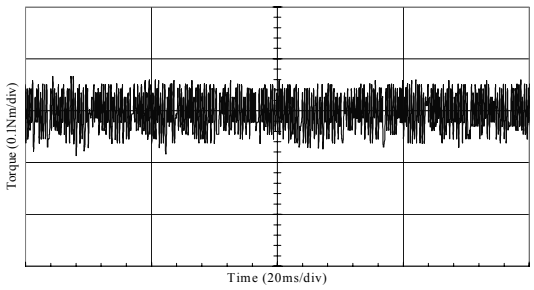


(e) Estimated electromagnetic torque

Figure 8. Experimental results for Motor 1 (1500rpm).

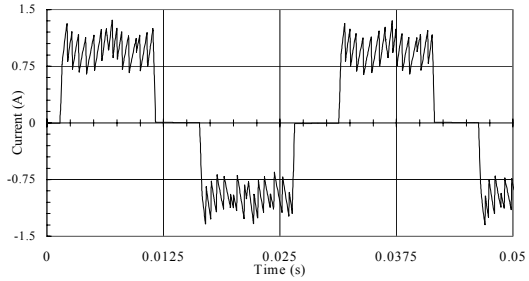


(c) Phase current

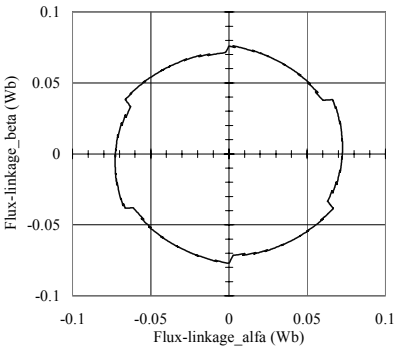


(d) Locus of stator flux-linkage

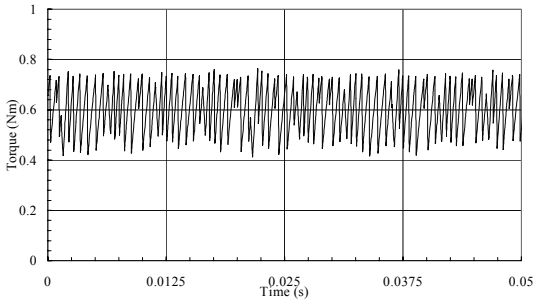


(e) Electromagnetic torque

Figure 9. Simulated results for Motor 2 (400rpm).

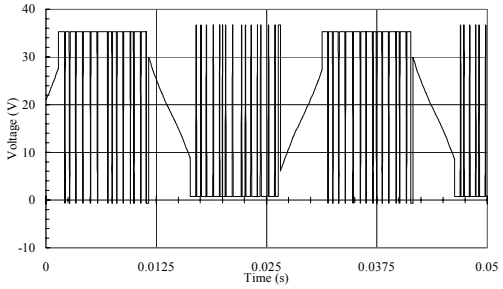


(a) Phase winding terminal to ground voltage

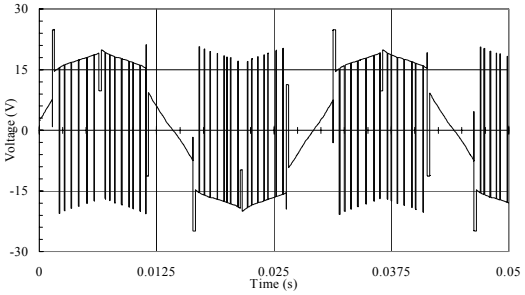


(b) Phase voltage

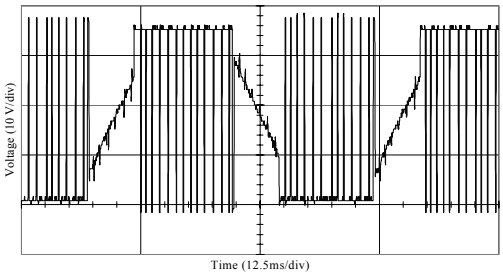


(a) Phase winding terminal to ground voltage

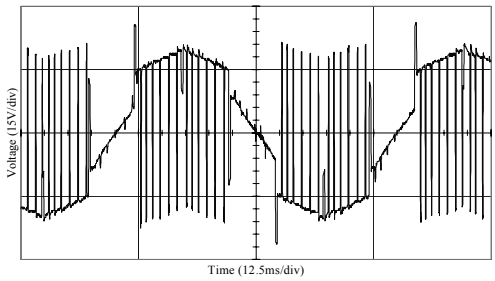


(b) Phase voltage

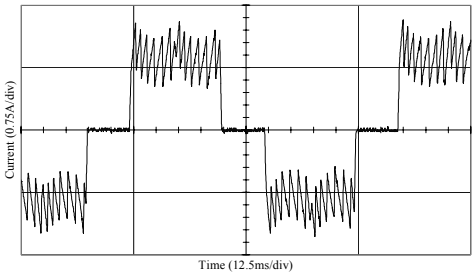


(c) Phase current

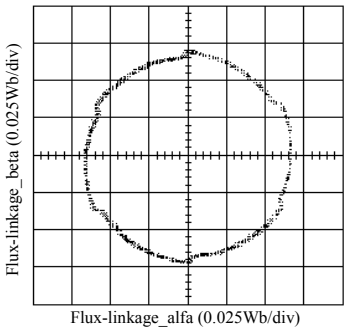


(d) Locus of stator flux-linkage

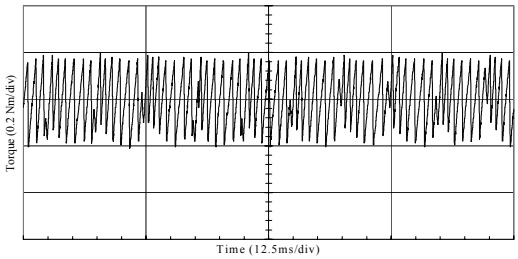


(e) Estimated electromagnetic torque

Figure 10. Experimental results for Motor 2 (400rpm).

## IV. CONCLUSIONS

Direct torque control has been applied to a BLDC drive, and its utility has been validated by simulations and experiments. The main difference between the direct torque control of BLAC and BLDC drives is in the estimation of torque and the representation of the inverter voltage vectors. It has been shown that DTC is capable of instantaneous torque control and reducing the torque pulsations in BLDC drives, and, thereby, of enhancing performance.

## REFERENCES

[1] P. J. Sung, W. P. Han, L. H. Man, F. Harashima, "A new approach for minimum-torque-ripple maximum-efficiency control of BLDC motor," *IEEE Transactions on Industrial Electronics*, Vol.47, Feb. 2000, pp.109-114.

[2] C. French, P. Acarnley, "Direct torque control of permanent magnet drives," *IEEE Transactions on Industry Applications*, Vol.32, Sep/Oct 1996, pp. 1080-1088.

[3] T. S. Low, K. J. Tseng, K. S. Lock and K. W. Lim, "Instantaneous torque control," *Fourth International Conference on Electrical Machines and Drives*, 13-15 Sept. 1989, pp.100-105.

[4] T. S. Low, K. J. Tseng, T. H. Lee, K. W. Lim and K. S. Lock, "Strategy for the instantaneous torque control of permanent-magnet brushless DC drives," *IEE Proceedings on Electric Power Applications*, Vol.137. Nov. 1990, pp.355-363.

[5] T. S. Low, T. H. Lee, K. J. Tseng and K. S. Lock, "Servo performance of a BLDC drive with instantaneous torque control," *IEEE Transactions on Industry Applications*, Vol.28, 1992, pp.455-462.

[6] Kang Seog-Joo, Sul Seung-Ki, "Direct torque control of brushless DC motor with non-ideal trapezoidal back-emf," *IEEE Transactions on Power Electronics*, Vol.10, Nov. 1995, pp.796-802.

[7] Se-Kyo Chung, Hyun-Soo Kim, Chang-Gyun Kim, Myung-Joong Youn, "A new instantaneous torque control of PM synchronous motor for high-performance direct-drive applications," *IEEE Transactions on Power Electronics*, Vol.13, No.3, May, 1998, pp.388 –400.

[8] P. C. Krause, *Analysis of Electric Machinery*. New York: McGraw-Hill, 1987.

[9] V. Gourishankar, *Electromechanical Energy conversion.* Scranton, Pennsylvania: International textbook company, 1965.

[10] B. H. Ng, M. F. Rahman, and T. S. Low, "An investigation into the effects of machine parameters on torque pulsation in a brushless dc drive," *Proceeding of IEEE IECON*, 1988, pp. 749–754.

[11] L. Zhong, M. F. Rahman, W. Y. Hu and K. W. Lim, "Analysis of direct torque control in permanent magnet synchronous motor drives," *IEEE Transactions on Power Electronics*, Vol. 12, No.3, May, 1997, pp.528-536.